photonics

MDPI

Review

Polymer Materials for U-Shaped Optic Fiber Sensors: A Review

Patryk Sokołowski [1,*], Jacek Łubiński [2], Paweł Wierzba [1], Jakub Czubek [1], Piotr Miluski [3], Filip Janiak [1,4], Shanyue Guan [5] and Małgorzata Szczerska [1,4]

[1] Department of Metrology and Optoelectronics, Faculty of Electronics, Telecommunications and Informatics, Gdańsk University of Technology, 11/12 Narutowicza Street, 80-233 Gdańsk, Poland; jakub.czubek@pg.edu.pl (J.C.); malszcze@pg.edu.pl (M.S.)
[2] Department of Machine Design and Vehicles, Faculty of Mechanical Engineering and Ship Technology, Gdańsk University of Technology, 11/12 Narutowicza Street, 80-233 Gdańsk, Poland; jacek.lubinski@pg.edu.pl
[3] Faculty of Electrical Engineering, Bialystok University of Technology, Wiejska 45D Street, 15-351 Bialystok, Poland
[4] Sussex Neuroscience, School of Life Sciences, University of Sussex, Brighton BN1 9RH, UK
[5] Technical institute of Physics and Chemistry, Chinese Academy of Sciences, 29 Zhongguangcun East Road, Beijing 100190, China
* Correspondence: patsokol@pg.edu.pl

Abstract: Fiber optic sensors have gained popularity over the last few decades. This is due to their numerous advantages, such as good metrological parameters, biocompatibility and resistance to magnetic and electric fields and environmental pollution. However, those built from glass fiber have one main disadvantage—they are fragile, meaning they can be easily damaged, even by the presence of vibration. Due to the great progress made by material research recently, it is possible to build such a sensor with polymer fibers instead. Although those fibers have worse transmission parameters compared to telecommunication fibers, they provide the possibility to realize flexible fiber optic sensors. Taking into consideration other advantages of such fibers, including biocompatibility, electromagnetic resistance and even, biodegradation characteristics, as well as there being a variety of materials we can use, it can be seen that those materials are beneficial to produce fiber optic sensors. This paper aims to provide researchers with guidelines on the factors to consider when choosing a material for bent fiber optic sensors, depending on the application.

Keywords: polymer; optical fiber; fiber optic sensing

check for updates

Received: 13 December 2024
Revised: 4 January 2025
Accepted: 6 January 2025
Published: 10 January 2025

Citation: Sokołowski, P.; Łubiński, J.; Wierzba, P.; Czubek, J.; Miluski, P.; Janiak, F.; Guan, S.; Szczerska, M. Polymer Materials for U-Shaped Optic Fiber Sensors: A Review. *Photonics* **2025**, *12*, 56. https://doi.org/10.3390/photonics12010056

Copyright: © 2025 by the authors. Licensee MDPI, Basel, Switzerland. This article is an open access article distributed under the terms and conditions of the Creative Commons Attribution (CC BY) license (https://creativecommons.org/licenses/by/4.0/).

1. Introduction

The polymer optical fiber (POF) market has shown steady growth for a number of years, with a compound annual growth rate of 11% between 2010 and 2019. The market consists of seven segments, including automotive, industrial, medical, military, office, home and architecture. In 2015, approximately 165,000 km of POFs were sold, mostly for applications in home (43%), automotive (30%) and industrial (18%) sectors. Data transmission at short distances is the most common application of POFs (51%), followed by illumination (46%) and fiber sensors (3%). In Europe, the home sector is negligible, and polymer optical fibers are applied mostly in automotive (67%) and industrial (29%) sectors, due to the lack of popularity of optical fiber illumination there (Figure 1) [1].

Compared to glass optical fibers, polymer optical fibers have different properties. Typically, POFs are multimode fibers, whose diameters of the core are in the range of 250 μm^{-1} mm, which are considerably larger than the 50 µm and 62.5 µm core diameters of the most popular step-index and gradient index glass optical fibers. The attenuation of

POFs is higher than that of glass optical fibers, typically over 0.1 dB/m for most common Poly (methyl methacrylate) (PMMA) POFs [2] vs. ~0.02 dB/km for a glass optical fiber [3], reaching its minimum at 600–700 nm, making POFs unsuitable for long-distance signal transmission. On the other hand, polymer materials have higher flexibility. This feature makes it possible to produce sensors in a variety of shapes [4,5] that are difficult to attain in glass optical fibers.

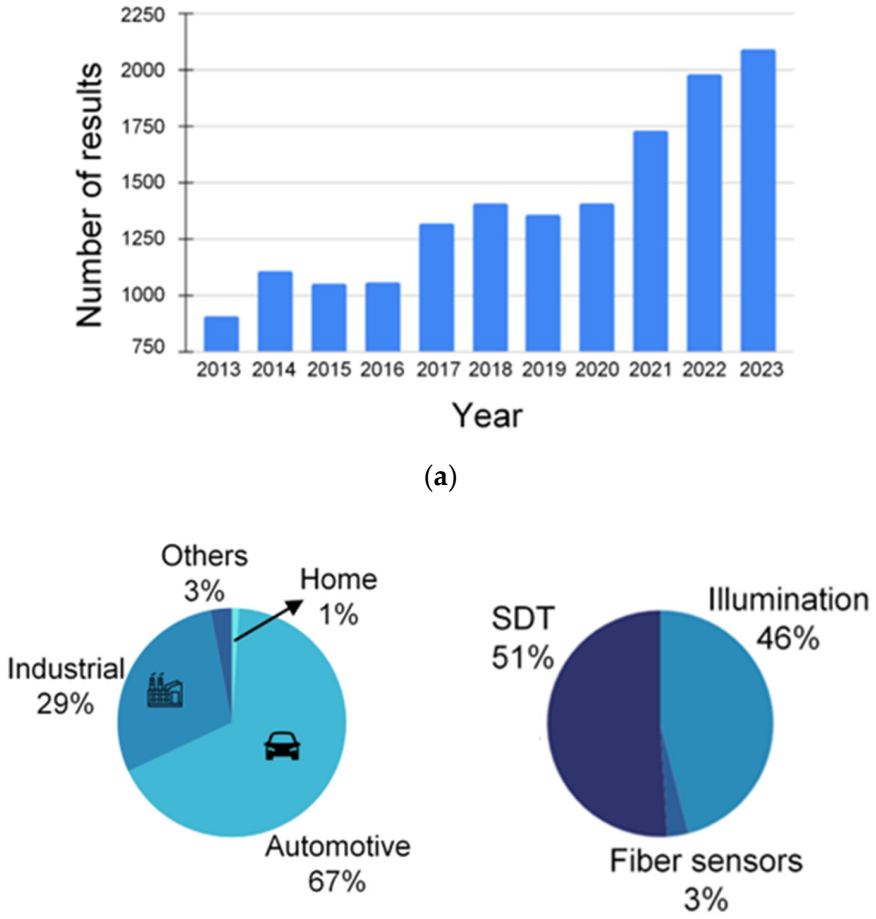


Figure 1. (**a**) Number of results on query "POF sensor" in Google Scholar [6], (**b**) representation of specific business in overall POFs production, (**c**) participation of selected applications in overall scheme. SDT stands for Short Distance Transmission.

Optical fibers can be used for the transmission of information and for sensing several physical, chemical and biological quantities. Based on a Google Scholar search for the query "POF sensor", it is apparent that the number of results has increased over the last years, as shown in Figure 1a. The spikes in interest in POFs observed during 2016–2017 and 2020–2021 are likely attributable to the introduction of fiber optic-based technologies in the automotive industry, the growing interest in 3D printing and the potential for manufacturing POFs using similar methods, as well as the increasing focus on utilizing POFs in medical diagnostics, particularly in response to the COVID-19 pandemic.

The use of POFs in sensing is increasing and its field of application is expanding. There are numerous benefits of polymer fibers, including being lightweight, having high flexibility, biocompatibility, being resistant to electromagnetic interference, having a dielectric structure and being suitable for performing direct and real-time optical measurements. Polymer optical fibers can be applied in environments that are not suited for electric con-

ductors and electronic components [7] due to their immunity to high electric and magnetic fields (Figure 1b). POFs find applications in medicine, e.g., in photodynamic therapy (PDT) or optogenetic stimulation [8], and optical fiber sensing. Polymer optical fibers are also suitable for portable handheld sensors that eliminate the requirement to gather samples on-site and conduct the analysis in a laboratory setting. A simple optoelectronic sensor requires only a source of optical radiation (e.g., an LED), a fiber and a photodetector, followed by a microcontroller with a display [9]. However, the applications of POFs are mainly focused on short-distance transmission and illumination rather than on the development of new sensors (Figure 1c). New biodegradable materials for POFs are constantly being developed based on biodegradable materials [10]. This is not only to the advantage of the natural environment but also to benefit an increasing number of new applications. A biodegradable fiber can be implanted into a patient's body for the duration of the treatment in the bodily tissues and will degrade naturally in a harmless manner after the treatment has been completed [11].

The range of materials that can be used in polymer optical fibers for sensing applications is continually expanding. At present, the most commonly used material for polymer optical fiber is PMMA [2], the main advantage of which is a relatively low cost. The alternatives to PMMA are low-loss amorphous fluorinated polymers (CYTOP) [12], water absorption-resistant materials like cyclic olefin polymers (TOPAS and ZEONEX) [13,14], materials with excellent impact strength like polycarbonate (PC) [15], which can be printed in 3D, and biodegradable materials such as poly-D,L-Lactic Acid (PDLLA) [10]. New materials are being developed for sensing POFs in order to improve their optical and mechanical properties and to provide resistance to selected chemical compounds, in order to enhance the operating temperature range or to tailor the biodegradability of the POFs.

Several types of optical fiber sensors using diverse operation principles can be implemented using polymer optical fibers. In particular, sensors reported in the literature use intensity [16], interferometry [17], Bragg gratings [18] and optical time domain reflectometry [19]. The class of intensity optical fiber sensors known as U-shaped sensors was selected for this review, as it apparently has the most diverse range of POF types that can be employed as its sensing elements.

The purpose of this paper is to review polymer materials that can be used in the sensing part of U-shaped optical fiber sensors. The principles of the operation of U-shaped sensors are outlined in Section 2. Following this, the applications of U-shaped optical fiber sensors are briefly discussed in Section 3. The review of polymer materials for sensing POFs is presented in Section 4, while Section 5 contains conclusions and a brief discussion.

2. POF U-Shaped Sensor Principles

An optical fiber consists of a core, usually with a circular cross-section, where light is guided, and embedded in a cladding, as shown schematically in Figure 2. Both core and cladding are made from isotropic dielectric materials with a low attenuation of transmitted light.

The propagation of light in an optical fiber depends on the size of the core diameter of the cladding as well as of the refractive indices of the core and cladding materials, n_1 and n_2, respectively.

An isotropic material's refractive index (RI) is determined by the ratio of the velocity of light in a vacuum to the velocity of light in the material [20], such as the following:

$$n = \frac{c}{v}, \tag{1}$$

where c—velocity of light in vacuum and v—velocity of light in the material. While the value of n_1 is of secondary importance in most data-transmission applications, n_2 is one of the most crucial parameters of fibers used for sensing purposes, due to the necessity of internal reflection within the fiber.

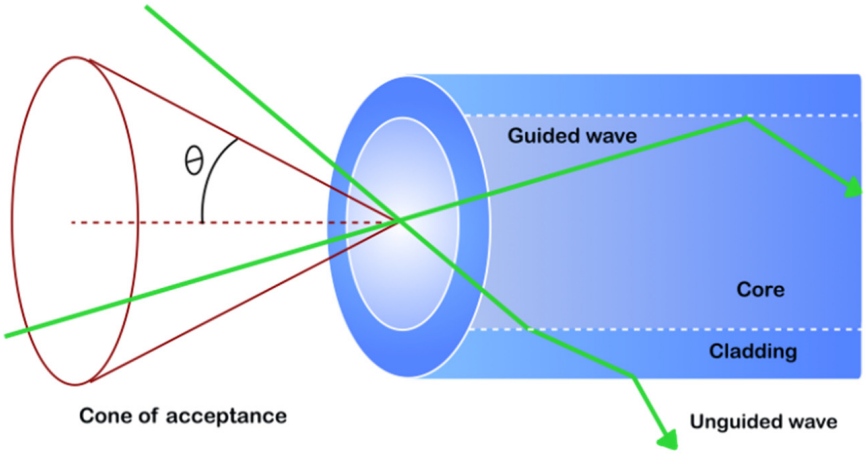


Figure 2. Guiding light into the fiber, where θ is the angle of the cone of acceptance.

A wave incident on the end face of the fiber becomes a guided wave when its direction of propagation is within the cone of acceptance, as shown in Figure 2. Otherwise, it becomes an unguided or evanescent wave (EW). The acceptance angle θ of the fiber is defined as the following:

$$\theta = sin^{-1}(NA), \tag{2}$$

where NA is the numerical aperture of the fiber, defined as the following:

$$NA = \sqrt{n_1^2 - n_2^2}, \tag{3}$$

where n_1—refractive index of the core and n_2—refractive index of the cladding [21].

For the fiber to operate properly, n_1 must be greater than n_2 in order to preserve the phenomenon of total internal reflection. Numerical aperture is used as a measure of the light-gathering properties of the fiber. The greater the NA, the greater the acceptance angle θ and the wider the acceptance cone, allowing more waves into the fiber, as shown in Figure 2.

Any wave propagating in the fiber has to satisfy its characteristic equation [22]. The number of its solutions is finite, and each solution is called a mode. The quantity of modes propagating in a fiber depends on the radius a of its core, the refractive indices n_1 and n_2 of its core and cladding, respectively, and the wavelength λ of light propagating in the fiber.

For the given refractive indices n_1 and n_2, it is possible to reduce the radius of the core a to a value for which only one mode propagates in a fiber for any wavelength λ longer than the cutoff wavelength λ_c given by [21]:

$$\lambda_c = \frac{2\pi}{2.405} a \cdot NA. \tag{4}$$

A fiber in which only one mode can propagate in the operating wavelength range of the fiber is called a single-mode fiber, while a fiber in which several modes can propagate in the operating wavelength range is called a multi-mode fiber.

Attenuation restricts the distance a signal can propagate through the fiber before the optical power deteriorates excessively. Several factors can cause attenuation, like material

absorption, scattering in material or bending [21]. Attenuation coefficient α, expressed usually in dB/km or dB/m is defined as the following:

$$\alpha = \frac{-10}{L} \log_{10}\left(\frac{P_{out}}{P_{in}}\right), \tag{5}$$

where L—distance, P_{in}—input power and P_{out}—output power.

Most U-shaped sensors are intensity sensors, operating using measurement-induced intensity changes. These changes may be caused either by changing the propagation conditions of the fiber or by the absorption of the evanescent field, as described in Sections 2.1 and 2.2, respectively.

2.1. Sensing with Propagation Conditions in the Fiber

Light propagating in an unperturbed POF is attenuated according to (5). However, when a section of cladding is removed and replaced with another liquid or solid material that exhibits little absorption, the propagation conditions in that fiber segment start to depend on the refractive index of that material [23]. In particular, when its refractive index is greater than that of the cladding, the NA decreases (c.f. (3)), and some light becomes unguided and is coupled to the outside medium. The amount of light coupled depends on the length of the section. Additionally, the bending of the fiber into a U shape introduces additional changes in the propagation conditions, making the sensor more sensitive. Sensitivity can also be tailored by tapering [24] or polishing [25] the core. Coatings with a thickness well below the wavelength of the light propagating in the fiber can be applied on the core to protect it from the environment in which the sensor operates without substantially changing the properties of such sensors [26,27].

2.2. Sensing with Evanescent Field

When light is transmitted in an optical fiber, part of its energy, called an evanescent wave, propagates in the cladding. When EW extends into the medium surrounding the core, its amplitude E decays exponentially:

$$E = E_0 * e^{\frac{-z}{dp}}, \tag{6}$$

where E_0 is the amplitude of the field at the surface of the core, z is the distance from the surface of the core and dp is the penetration depth, which can be expressed as:

$$dp = \frac{\lambda}{2\pi\sqrt{n_1^2 sin\theta - n_2^2}}, \tag{7}$$

where λ is the wavelength in vacuum and θ is the incident light angle [28].

Interaction between the evanescent wave and the substance surrounding the fiber takes place when a significant part of energy propagating in this wave extends into that substance. This interaction can be promoted by the partial or complete removal of the cladding of the fiber, as shown in Figure 3a. Increased evanescent wave power enhances sensitivity by providing more evanescent waves to interact with the surrounding medium [29]. As the energy loss of the evanescent wave depends, in particular, on the length of the sensing fiber section, the refractive index and the absorption coefficient of the surrounding substance, changes in the two latter quantities can be detected by measuring the intensity of light exiting the sensing fiber section.

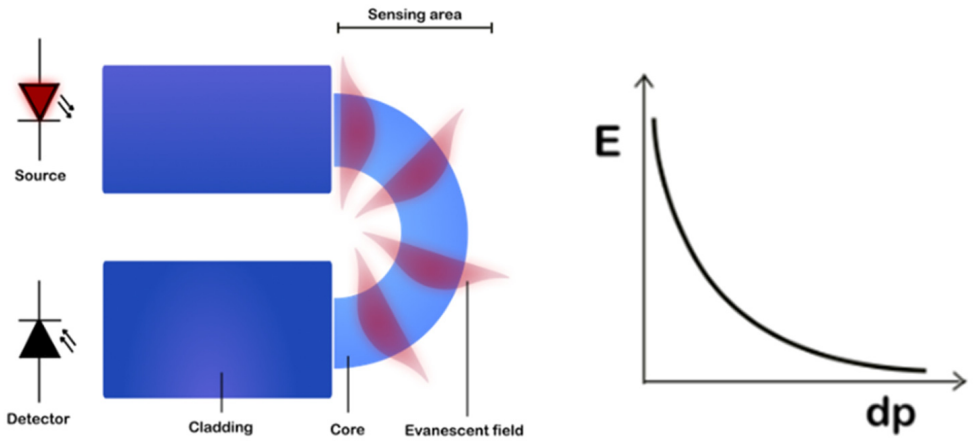


Figure 3. (**a**) Schematic representation of evanescent waves for U-shaped fiber sensor and (**b**) energy of evanescent field *E* as a function of the distance from the surface of the core *dp*.

2.3. U-Shaped Fabrication

Fire or another heat source can be used to soften the optical fiber and bend it into a suitable shape that will be retained after it cools down. Parameters such as the bend radius or angle could be hard to repeat, so a mold is proposed, e.g., in the form of a glass tube [30] or curved blunt needles [31]. In addition, the glass tube can then be filled with glue to help retain the shape of the fiber and form a structural package for the sensor. Another method that can help control the parameters of bending is to use heated metal molds [32]. In general, it can be stated that the use of thermoplastic polymers as material bases for U-shaped fiber optic sensors is well justified regarding the fundamental issue of forming the shape of the active part of the sensor. The properties of the materials in this group allow for a relatively straightforward execution of the bending. Also, it is possible to achieve shape retention by heat treatment which relaxes the internal stresses and decreases the tendency for fiber re-straightening.

Cladding removal can be performed mechanically, by stripping and polishing, or using chemical agents, such as acetone or ethyl acetate [9], depending on the materials of core and cladding.

Fiber Bragg gratings (FBGs) can be used to aid and modify the performance of U-shaped fiber optic sensors [33]. The FBG is a type of optical filter that reflects specific wavelengths of light and transmits all others in an optical fiber. It is created by inducing a periodic variation in refractive index changes within the core of an optical fiber, which leads to constructive interference of light at the Bragg wavelength and destructive interference at other wavelengths. FBGs are often used as sensing elements in various applications such as temperature, pressure, strain and vibration sensing. The combination of U-shaped fibers and FBGs exhibits an increase in signal power while grating is in stretching mode and therefore located on the outer part of the bent fiber [34].

3. Applications for U-Shaped POF

U-shaped POF sensors find applications in various fields, such as biosensing, chemical sensing and physical sensing [35–37]. The U-shaped design of the fiber allows for a larger sensing area and increased sensitivity compared to straight fiber sensors. Some important sensor applications are shown in Table 1.

Table 1. Selected application of polymer optic fibers U-shaped sensors.

Application		Metrological Parameter	Material	Ref.
Physical	Temperature	Temp. range: 30–80 °C Sensitivity: 0.596 nm/°C	PMMA coated with PDMS	[38]
	Humidity	Range: 35–90% RH Sensitivity: 0.0194 V/%RH	PMMA coated with ZnO	[39]
	RI	Range: 1.34–1.37 RIU Sensitivity: 1258 nm/RIU	PMMA coated with PDMS	[38]
Chemical	pH	Range: 4.5 to 12.5 Resolution: 0.02 pH within the pH range: 7.5–12.5	n.r. *	[40]
	Glucose	Lowest detected concentration: 1.2 mmol L^{-1}	p (AM-co-PEGDA) coated with Ca-alginate	[41]
	Water salinity	Concentration: 0–25% v/v	PMMA	[42]
	Ethanol	Concentration: 0.00633 to 80% v/v LOD of 9.7 × 10^{-6} RIU	PMMA	[31]
	Formaldehyde Vapor	Concentration: 5% to 20% Sensitivity: 0.00543 V/%	PMMA coated with ZnO	[43]
Biomedical	*E. coli*	10^4–10^8 CFU/ml	PMMA	[37]
	Respiratory rate sensor	Breaths per minute	CMC	[44]

* n.r.—non recorded.

A U-shaped fiber optic sensor can be used to identify variations in the refractive index of its surrounding environment. The probe can be dipped into a solution with varying refractive indices, typically below the RI of the core of the fiber. This sensing principle can be used for the measurement of all quantities that modify the RI of the solid or liquid material surrounding the core of the sensing fiber.

In particular, U-shaped sensors can be applied to measure temperatures in the range of 30–55 °C and find the location of the heat source [45]. In chemical sensing, they can be employed for the measurement of water salinity [42], sugar or alcohol concentration in water [31] or the detection of contaminants in water. More advanced applications of U-shaped sensors rely on the functionalization of the surface of the core of the sensing fiber. An example sensor used a fiber whose surface was functionalized with silver nanoparticles and was tested in an alcohol solution [46].

U-shaped sensors in biological applications were used for the detection of bacteria in tap water by RI measurements in the range of 1.33–1.39 or 0.06 RIU, with the sensing region tapered to achieve a higher sensitivity level [24]. Immunosensors were also demonstrated. In particular, biosensors with a U shape were fabricated for the detection of copper ions in blood serum with a limit of detection of 7.5 fM in tap water [47]. The sensors were functionalized with immunoglobulin G as the receptor molecule and copper concentration measurement was performed by measuring the change in absorbance. An immuno-biosensor of the chikungunya protein was demonstrated using a system functionalized with gold nanoparticles and an antibody as a label for detection, relying on the measurement of absorbance change with a detection limit of 0.52 ng mL^{-1} [48]. For bacterial detection, U-shaped fiber sensors were functionalized with antibodies and were tested for *E. coli* detection within the range of 10^4–10^8 CFU/mL [37].

PMMA is the most common material of choice when using the U-shaped sensor. Constructing a sensor with a new polymer material can lead to the creation of novel sensors and the finding of new applications. The development of technologies for functionalization

and geometric modification of fiber optics offers numerous possibilities for the modification and optimization of U-shaped sensor's performance.

4. Materials for Polymer Optic Fibers

Polymer optical fibers (POFs) are used as an alternative to glass optical fibers (GOFs). Advantages of POFs include a low-attenuation window in the visible wavelength range (400–700 nm) and flexibility, especially in fibers of larger diameters (~1 mm). The main criteria for the selection of materials for optical fibers are the refractive index, melting point, proper flexibility, mechanical strength and suitable resistance to the factors in the environment where the sensors operate. POFs can be manufactured from a wide range of polymeric materials, some of which, mentioned in this section, are collected in Table 2.

Table 2. Standard and novel materials for polymer optic fibers.

Conventional Polymer Optic Fibers (POFs)	Hydrogel Optical Fibers (HOFs)	Biopolymer Optic Fibers (BIOPOFs)	High-Performance Polymers (HPPs)	UV Acrylics, Polymers, Urethanes
Poly (methyl methacrylate) (PMMA) [48–57]	The poly (D,L-Lactic Acid) (PDLLA) [11,58]	Spider silk [59,60]	CYTOP [49,61–66]	UV-curable methacrylates [67]
Polycarbonate (PC) [50,54,68]	Poly (ethylene glycol) (PEG) [69,70]	Silkworm silk [59,71]	ZEONEX [72–75]	Methacrylate set with luminophores [76]
Polystyrene (PS) [54]	Polyethylene glycol diacrylate (PEGDA) [77]	Cellulose [78]	TOPAS [13,79]	UV polymer composite [80]
	Natural polymers (agarose, gelatin, cellulose derivatives) [77,78,81]			Rubbers, urethanes, silicones [77]
	Polyacrylamide (PAAm) [77]			

4.1. Conventional POFs

PMMA, also known as "Plexiglas", is the most commonly chosen material for POF fabrication and is widely available commercially [50]. PMMA is resistant to water and oil, but under humid conditions, PMMA tends to absorb water up to 2% [51]. The refractive index of PMMA is 1.49 [51–54]. The PMMA material performs well in the visible spectrum with the optical windows in the range of 400–700 nm and for infrared, at ~850 nm. the standard working temperature ranges from −40 to +85 °C, and at 130 °C, the material approaches its melting point [52,54]. For high-temperature applications, the material used for the optical fiber must be capable of functioning at temperatures exceeding 100 °C. PMMA can be used in 3D printing; however, the use of this technology results in high transmission losses experienced by the final product [53]. The tensile strength reaches approximately 76 MPa [54]. The material exhibits biocompatibility [54] and a good compatibility with the human tissue [56]. After 15 days of PMMA exposure via a 40 W UV lamp (290–315 nm), a transmittance reduction of 5% occurs [57].

Commercially, standard PMMA POFs are multi-mode, with a high numerical aperture (*NA*) (~0.5), which makes it easier to connect to low-cost sources and detectors. The most popular size of 1 mm is dominant on the market, but different sizes are also available, ranging from 0.25 mm to 1 cm. The attenuation profile of a typical PMMA fiber is shown in Figure 4a. The most common fiber cladding material is modified (fluorinated) PMMA polymer, which has a lower refractive index than the core (RI ≈ 1.35). In POFs, the cladding represents usually around 2–5% of the fiber diameter.

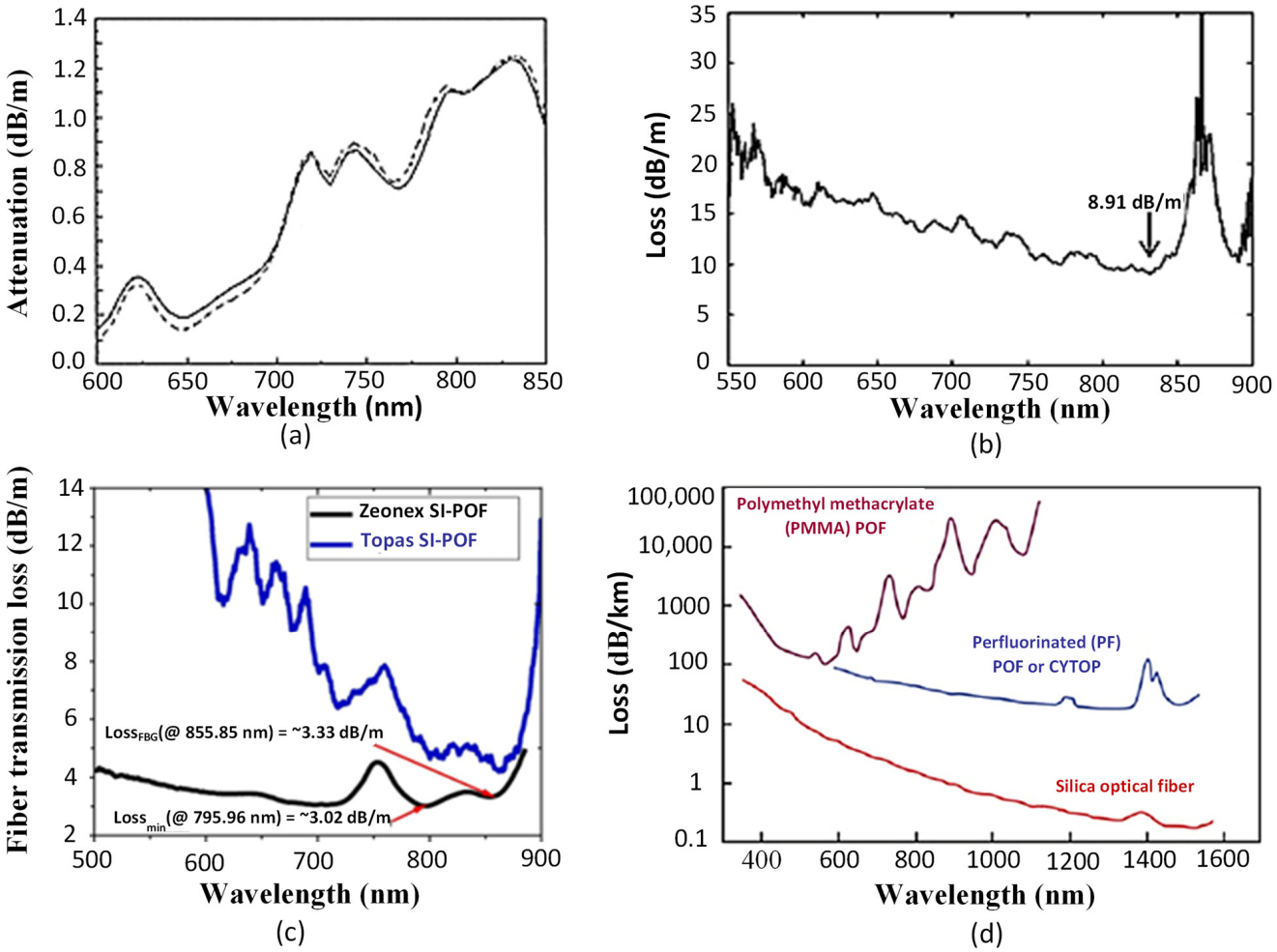


Figure 4. (**a**) Attenuation spectrums of sample 7 PMMA POF (-) before and (. . .) after surface fluorinating (reproduced with permission from Ref. [2], Wiley Copyright 2024); (**b**) transmission loss fiber made by PC material (adapted with permission from [15], © The Optical Society); (**c**) transmission loss for SI-POF made with Zeonex and Topas materials (reproduced with permission Ref. [75], Elsevier Copyright 2024); and (**d**) attenuation of silica and polymer: PMMA and CYTOP fibers (based on ref. [49]).

Crystallizable polymers contain both crystalline and amorphous regions, but amorphous polymers are favored as a core material due to their uniform density. PC-based optical fibers have very similar RIs to the PS (1.58) and lower optical losses than PS, but higher compared to PMMA. PC also exhibits greater heat resistance. The higher glass transition temperature (Tg = 150 °C), which represents the temperature at which a material turns from a rigid state to a flexible state, allows PC to withstand a high operating temperature (up to 130 °C) [54].

The blend of the optical and mechanical attributes of PC makes it suitable for optical fiber applications. POFs made of polycarbonate have relatively large *NA*, as compared to other POFs, which can be explained by the high refractive index of PC. The PC fibers provide efficient short-range optical transmission within a visible range. The absorbance characteristic of the solid-core PC shown in Figure 4b suggests a greater absorbance between 800 and 900 nm. The average tensile strength is also similar to the PMMA material 62.0–64.3 MPa [5]. One disadvantage of PC is the tendency to yellow due to aging and losing transmission quicker than PMMA [82]. The relative transmission drops with aging several times quicker than in PMMA fibers. The material can be used for 3D printing and also fiber fabrication [83]. The PC material can be used for fiber core fabrication in

various shapes [68]. Multi-mode PC polymer optical fibers offer easier coupling with light transmitters and receivers using economical connectors [50]. Currently, fiber optics made of PC have been replaced on the market by POFs made of PMMA.

Polystyrene (PS) material is suitable for making optical fibers, but its optical properties are inferior compared to the mentioned synthetic polymers fibers. Therefore, there has been no reason to replace the PMMA POFs with PS fibers.

A U-shaped PMMA POF biosensor coated with gold has been developed for the detection of E. coli. The POF functions as a refractive index sensor without the necessity of cladding removal. U-shaped probes coated with gold with thicknesses of up to 18 nm exhibit behavior comparable to uncoated probes, with the bending loss being the primary sensing mechanism. Probes coated with a thin layer of gold, below 50 nm, are ineffective for that sensing application. In contrast, probes coated with 70 nm and 100 nm of gold demonstrate the predominance of surface plasmon resonance (SPR) effects, enabling the biosensor to detect bacterial concentrations as low as 1.5×10^3 CFU/mL [84].

M. Lomer et al. fabricated a refractometric sensor based on PMMA POF for measuring power losses in liquids. The operating principle relies on induced losses occurring in the transition region of a curved side polished POF [25]. Ara Rashid et al. presented the POF composed of a PMMA core and a fluorinated polymer clad with refractive indices of 1.49 and 1.41, respectively. They tested the sensor for *E. coli* [85]. Shumin Wang et al. developed a double-sided polished U-shaped POF sensor made of PMMA for RI application. The sensor promises great potential in liquid RI, measuring from 20 to 50 °C [32]. A PMMA-based U-shaped POF sensor has been applied in real-time monitoring systems and utilized for detecting scale deposition in hot spring water sources [86].

4.2. Hydrogel Optical Fibers (HOFs)

Hydrogels offer versatility in adjusting the optical and mechanical properties of the material by manipulating the polymer-to-water ratio, resulting in transparency, flexibility and stability [83]. Common HOFs fabricate raw materials, agarose, alginate, gelatine, cellulose derivatives, PVA, poly (ethylene glycol) (PEG), Polyethylene glycol diacrylate PEGDA and polyacrylamide (PAAm) [77].

For the poly (ethylene glycol) (PEG)-based hydrogel fiber, the refractive index can be changed by the precursor concentration. The reported PEG fiber with alginate hydrogel clad has low-loss light guiding (<0.42 dB/cm) over the entire visible spectrum [69]. The obtained core size ranges from 250 to 1000 μm, and a different size of cladding depends on the number of layers. Hydrogel fiber can be soft, have low cytotoxicity and have good selling stability, which makes them suitable for use in photomedical applications in tissues, like photothermal and photodynamic therapy [70].

Currently, PEDGA is a widely studied synthetic polymer material due to its broad range of applications, attributed to its key properties such as nontoxicity, softness, and suitability for use in implantable devices. This material is particularly well-suited for biomedical applications due to its simple gelation process with divalent cations [77].

The fibers derived from cellulose-based materials exhibit renewability, biocompatibility and biodegradability. The 1.6 dB/cm attenuation coefficient was measured at 637 nm for reported fiber modes of carboxymethyl cellulose (CMC) hydrogels without cladding. These optical fibers found successful applications in touch sensing and monitoring respiratory rates. Furthermore, the high-speed signal transmission at 150 Mbit/s was demonstrated over short distances using CMC fibers [44].

The poly (D,L-Lactic Acid) (PDLLA) is another suitable natural material for the relatively fast degradation required of POF applications. Degradation over time has been reported for fibers made from PDLLA material. A decrease of over 80% was observed

within 3 months. Similarly to other degrading optical fibers, the degradation time depends on parameters such as the material's thickness and morphology. Larger-diameter fibers tend to degrade faster than those with smaller diameters. Optical parameters for PDLLA fibers are as follows: attenuation of 0.16 dB/cm at 650 nm and 0.13 dB/cm at 850 nm [11].

Biodegradable POFs with a faster degradation time and improved transmission properties have been reported. By creating a fiber with a core made from poly (D,L-lactic-co-glycolic acid) and a cladding made from poly (D,L-lactic acid), the lowest attenuation of 0.26 dB/cm at 950 nm and weight loss of 91% over 3 months was achieved [58].

Hydrogel optical fibers (HOFs) exhibit several advantages, including flexibility, low cytotoxicity and excellent structural stability. However, their primary limitation is high optical attenuation, which restricts effective light transmission to a few tens of centimeters. This poses a significant challenge, particularly for applications requiring longer transmission distances. To address this issue, ongoing research is focused on the development and implementation of novel materials that can enhance the optical properties of HOFs.

4.3. Biopolymer Optic Fibers (BIOPOFs)

Environmental factors have attracted cellulose and its derivatives as new biopolymers for BIOPOF applications [81]. Cellulose has excellent biocompatibility and can be blended with another biopolymer of spider silk which is also biocompatible and has shielding properties to make novel POFs as a promising material in medical applications.

Due to optical characteristics, those materials exhibit a promise for their utilization in optoelectronic devices. Besides fiber fabrication, cellulose and its derivatives have found versatile applications including OLED technology, flexible touch displays and solar cells [87]. Goudbut et al. developed a dual-core fiber structure with cellulose butyrate tubes as core and shell materials. This was achieved by utilizing two types of biodegradable cellulose with differing refractive indices, enabling the fabrication of the optical fiber. This approach leverages the refractive index contrast between the materials to guide light effectively, while maintaining biodegradability and environmental sustainability [88]. An optical fiber tailored for water-sensing applications was fabricated through the direct processing of cellulose, as reported by Orelma et al. Regenerated cellulose was dissolved in the ionic liquid, coagulated in water to form a regenerated fiber and, subsequently, coated with cellulose acetate. The resulting BIOPOFs exhibited minimal attenuation of 5.9 dB/cm at a wavelength of 1130 nm [10]. Cellulose-based optical fibers have great potential, through their biocompatibility and low environmental impact; unfortunately, more research is needed to improve optical properties [78].

Another notable biopolymer material is silk, which can be derived from silkworms or spiders [59,60]. An optical structure based on silk derived from silkworms was produced by Omenetto et al. The material exhibited toughness and excellent optical transparency in the visible range, with a transmittance of approximately 92% [59]. Furthermore, Parker et al. used silkworm silk protein hydrogels for bioprinting it on a borosilicate glass substrate with a lower refractive index than the silk protein fiber-making waveguide [71]. These studies combined a similar approach of using surrounding media with a lower refractive index.

4.4. High-Performance Polymer POFs (HPPPOFs)

Perfluorinated polymer material known as CYTOP can operate in 200 to 2000 nm and achieves a ~0.2 dB/m attenuation [49]. This makes it a better material for the transmission of telecommunication signals compared to PMMA (Figure 4d). The CYTOP refractive index equals 1.34 at 584 nm [61] and has a tensile strength of 41–49 MPa with practically no water absorption [62]. Fiber made with CYTOP is "GigaPof" manufactured by Chromis

Fiberoptic in the USA. CYTOP material has better transmittance compared to PMMA. The CYTOP polymer was developed with the aim of mitigating the limitations imposed by molecular vibrations in the near-infrared (NIR) region. Notably, the C-H and O-H bond vibrations, which typically appear within the 1100–1700 nm range, pose a significant challenge for applications requiring high transparency in this spectral window. To overcome this, researchers proposed substituting hydrogen atoms with heavier isotopes such as fluorine in the CYTOP structure. This substitution effectively shifts the vibrational modes of the C-F bond toward longer wavelengths, thereby reducing their impact in the NIR range. As a result, CYTOP exhibits enhanced performance, expanding the potential applications of polymer optical fibers (POFs) in this critical spectral region [63]. Due to a low refractive index, the material presents low signal dispersion [64], which makes this material the most suitable for communication applications. For this reason, the medium is mostly used for data transmission, but also in a long array of sensors [65]. CYTOP in use as a sensor most often uses a fiber Bragg grating for measuring temperature, strain and humidity [66]. Subsequent applications are structural health monitoring, in mechanical and civil engineering, rehabilitation and robotics [12].

Another example of worthy material for use in optic fibers is the Cyclo Olefin Polymer (Zeonex). It has good transparency, and its signal loss is relatively low in the visible range. Compared to PMMA, it exhibits a very low affinity to water, at least 30 times, but poor resistance to oils. The tensile strength for Zeonex is in the range of 63–70 MPa [72]. For fiber made of Zeonex, the minimum recorded loss is 2.34 dB/m at 690 nm and in near-infrared propagation, the loss increases significantly [73]. The refractive index is equal to 1.52 [74]. The Zeonex material is proper for multicore fibers and other high-quality microstructure fabrication in the fiber. Although a single-mode fiber can be fabricated from Zeonex, it exhibits higher minimum losses, recorded at 3 dB/m at 796 nm. The maximum operating temperature of 123 °C was recorded [75].

A material similar to Zeonex is Topas. The main difference between those two materials is their optical loss within the visual and NIR ranges (Figure 4c), which suggests that the fiber loss for Topas is higher in the visible range. Additionally, when compared to PMMA, Topas has lower water absorption < 0.01%. Some materials of the Topas group are resistant to short-term high-temperature exposure of up to 170 °C, but the melting point is above 190 °C. The refractive index of Topas material is 1.53 and the tensile strength for Topas is in the range of 46 MPa [13].

The single-mode step-index fiber fabricated with a Topas core and Zeonex cladding has a loss of 4.55 dB/m at 850 nm. Other single-mode step-index POFs available commercially experience high losses (500 db/m at 850 nm) [79].

A U-shaped fiber optic sensor for humidity with measurements in the range of 15–85% RH has been presented by Zhao et al. The sensor was fabricated by coating a single-mode optical fiber bent into a U shape with a layer of polyvinyl alcohol (PVA). The sensor achieved a sensitivity of 318 pm/%RH [89]. Another author attempts to improve the sensor by adding graphene quantum dots (GQDs) to the humidity sensor probe. The electrospun optical fiber coated with PVA–GQDs film on the surface of a U-shaped optical fiber has been explored, with experimental results showing the average sensitivity of transmission as −0.131 dB/%RH [90].

The functionalization of PMMA core U-shaped POFs with Polyethyleneimine (PEI) enables the release of amines for antibody fixation. By bending, the sensitivity was increased by contact between the curved sensor component and the biological sample is achieved. The sensor formed this way can be then used with the evanescent field technique for sensing. Escherichia coli concentrations of 10^8 CFU/mL and 10^4 CFU/mL were detected by this biosensor using the designed optoelectronic data-collecting device [91].

4.5. Other POFs (UV-Curable and Sol–Gel-Based Acrylics, Water-Based Polymers and Urethanes)

UV-curable, sol–gel-based acrylics (urethane acrylates, silicon acrylates, fluorinated acrylates and methacrylates) and water-based polymers (urethanes, rubber-based systems) have an important potential for POF applications in future. A. Evertz et al. [67] has developed a UV-curable and dip-coating technique (optically compatible coating, RI = 1.4 (Fospia/Efiron)) to apply cladding material onto previously extruded POF cores (PMMA, RI =1.49) with diameters of about 16 µm. They also mentioned that at least a 20 µm diameter is needed for a stable and continuous process. The best-measured attenuations were determined as 3 dB/m for fibers with a core diameter of 46 µm. Rune Inglev et al. developed POF sensors for dissolved oxygen sensing by phase fluorometry [76]. The sensing matrix (luminophore platinum-octa ethyl porphyrin and the luminophore coumarin to increase the brightness) is applied as a film on the PMMA fiber end-surface. This approach can be extended to other polymers and luminophores. The UV polymerization fabrication method is also used for polymer composite-based optical fiber sensor fabrication [80].

5. Discussion

Fiber optics are made with the core composition listed in Table 3, but to make a U-shaped sensor, not all materials will be suitable. Based on optical losses, the best choice seems to be CYTOP. Unfortunately, its low refractive index is associated with a low numerical aperture, which causes a low number of propagated mods. CYTOP is well suited for communication applications, but not for making U-shaped sensors that are based on propagation loss in a sensing area. On the other hand, choosing a PDLLA with losses of 11 dB/m may prove to be a problem. Losses at this level necessitate making the sensor as short as possible, using a high-power source and a sensitive detector. The high attenuation of PEGDA fibers means that light can only be guided for a few tens of centimeters.

Table 3. Comparison of material for POF U-shaped sensors.

Material	Refractive Index of Core	Optical Loss [dB/m]	Tensile Strength [MPa]	Glass Trans. Temp. [°C]	Ref.
PMMA	1.49 @850 nm	0.2 @650 nm	76	105–120	[51–53]
CYTOP	1.34 @589 nm	0.06 @850 nm	41–49	108	[61,62]
ZOENEX	1.52 @589 nm	2.34 @690 nm	63–70	139	[72–75,82]
PDLLA	1.45 @656 nm	11 @772 nm	n.r. *	58	[11,92]
PEGDA	1.46 @532 nm	40 @532 nm	2.8–9.5	26.3–51	[41,93,94]

* n.r.—non recorded.

Zoenex and PMMA have similar parameters when it comes to refractive index and tensile strength, but the optical loss for PMMA is a few fold lower. Therefore, PMMA seems to be the most suitable material for the manufacture of U-shaped POF sensors. An additional advantage is that the use of PMMA for POFs is the most popular [95]. The ranking of all mentioned materials based on their properties (from 1 to 5) is shown in Figure 5, where a higher rank indicates a higher property value. This representation allows for a straightforward comparison of these materials in terms of their potential applications.

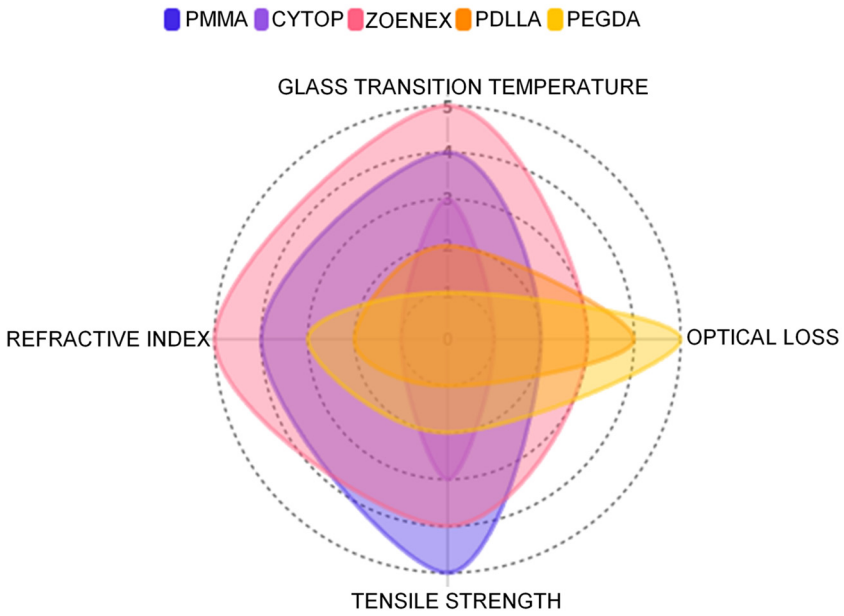


Figure 5. A spider plot showing the material properties of POFs presented in Table 3. The values are ranked from 1 to 5, where a lower property value corresponds to a lower rank.

6. Conclusions

Polymer optical fibers offer numerous benefits in sensing applications. In particular, their refractive index can be tailored to the needs of applications in a relatively broad range, while their size can also be varied. Their flexibility and the ability of some POFs to be produced using additive manufacturing techniques offer greater freedom in designing the sensing fiber section. The biocompatibility and biodegradability of selected POF materials, such as PMMA and PDLLA, facilitate their use in medical applications. Properly selected POFs are also able to operate in a relatively wide range of environmental conditions. POFs also provide numerous opportunities for geometrical modification or fabrication with additional layers of functional coatings.

In most cases, light can be easily coupled into POFs. This makes it possible to work with low-cost electronic components such as LEDs and photodiodes. The sensor created with POFs allows near real-time measurements. New materials for fiber fabrication are constantly being engineered, to achieve improved optical, chemical and mechanical properties. Through a variety of materials, fiber optics can be used in a variety of conditions, such as environment measurement or in biological tissues.

Author Contributions: Conceptualization, P.S. and M.S.; Methodology, P.S., M.S. and F.J.; Validation, M.S., J.Ł., P.W., P.M., S.G. and F.J.; Formal Analysis, P.S. and J.C.; Investigation, P.S. and J.C.; Resources, P.S., P.W., J.C., P.M., F.J., S.G. and M.S.; Data Curation, P.S. and J.C.; Writing—Original Draft Preparation, P.S. and J.C.; Visualization, P.S. and J.C.; Supervision, M.S.; Funding Acquisition, M.S., all the authors edited and approved the manuscript. All authors have read and agreed to the published version of the manuscript.

Funding: This work was financially supported by the DS programs of Faculty of Electronics, Telecommunications and Informatics of Gdańsk University of Technology for the support, specifically through the 7/1/2024/IDUB/III.4.1/Tc and 14/1/2024/IDUB/III.4.1/Tc grant under the TECHNETIUM Talent Management Grants program, as well as by the COST action CA21159.

Data Availability Statement: No new data were created or analyzed in this study. Data sharing is not applicable to this article.

Conflicts of Interest: The authors declare no conflicts of interest.

References

1. Kallweit, J.; Pätzel, M.; Pursche, F.; Jabban, J.; Morobeid, M.; Gries, T. An Overview on Methods for Producing Side-Emitting Polymer Optical Fibers. *Textiles* **2021**, *1*, 337–360. [CrossRef]
2. Chu, J.R.; Zhong, L.S.; Wen, X.M.; Xu, C.X. Study on Surface Fluorinating for Reducing Attenuation of Polymethyl Methacrylate Polymer Optic Fiber. *J. Appl. Polym. Sci.* **2005**, *98*, 2369–2372. [CrossRef]
3. Coring SMF-28 Product Information. Available online: https://www.corning.com/media/worldwide/coc/documents/Fiber/product-information-sheets/PI-1424-AEN.pdf (accessed on 7 February 2024).
4. Chu, F.; Yang, J. Coil-Shaped Plastic Optical Fiber Sensor Heads for Fluorescence Quenching Based TNT Sensing. *Sens. Actuators A Phys.* **2012**, *175*, 43–46. [CrossRef]
5. Xue, P.; Wu, B.; Bao, H.; Zheng, J. Screw-Shaped Plastic Optical Fibers for Refractive Index Sensing. *IEEE Sens. J.* **2020**, *20*, 5237–5242. [CrossRef]
6. Google Scholar. Available online: https://scholar.google.com/ (accessed on 27 February 2024).
7. Habel, W.R.; Krebber, K. Photonic Sensors Review Fiber-Optic Sensor Applications in Civil and Geotechnical Engineering. *Photonic Sens.* **2011**, *1*, 268–280. [CrossRef]
8. Cochrane, C.; Mordon, S.R.; Lesage, J.C.; Koncar, V. New Design of Textile Light Diffusers for Photodynamic Therapy. *Mater. Sci. Eng. C Mater. Biol. Appl.* **2013**, *33*, 1170–1175. [CrossRef]
9. Gowri, A.; Rajamani, A.S.; Ramakrishna, B.; Sai, V.V.R. U-Bent Plastic Optical Fiber Probes as Refractive Index Based Fat Sensor for Milk Quality Monitoring. *Opt. Fiber Technol.* **2019**, *47*, 15–20. [CrossRef]
10. Orelma, H.; Hokkanen, A.; Leppänen, I.; Kammiovirta, K.; Kapulainen, M.; Harlin, A. Optical Cellulose Fiber Made from Regenerated Cellulose and Cellulose Acetate for Water Sensor Applications. *Cellulose* **2020**, *27*, 1543–1553. [CrossRef]
11. Gierej, A.; Vagenende, M.; Filipkowski, A.; Siwicki, B.; Buczynski, R.; Thienpont, H.; Van Vlierberghe, S.; Geernaert, T.; Dubruel, P.; Berghmans, F.; et al. Poly(D,L-Lactic Acid) (PDLLA) Biodegradable and Biocompatible Polymer Optical Fiber. *J. Light. Technol.* **2019**, *37*, 1916–1923. [CrossRef]
12. Theodosiou, A.; Kalli, K. Recent Trends and Advances of Fibre Bragg Grating Sensors in CYTOP Polymer Optical Fibres. *Opt. Fiber Technol.* **2020**, *54*, 102079. [CrossRef]
13. TOPAS® COC Cyclic Olefin Copolymer. Available online: https://topas.com/wp-content/uploads/2023/05/TOPAS_Product-Brochure.pdf (accessed on 5 January 2025).
14. Zeonex Product Information. Available online: https://www.zeon.co.jp/en/business/enterprise/resin/pdf/200323391.pdf (accessed on 7 February 2024).
15. Stajanca, P.; Markos, C.; Nielsen, K.; Bang, O.; Stefani, A.; Krebber, K.; Fasano, A.; Woyessa, G.; Rasmussen, H.K. Fabrication and Characterization of Polycarbonate Microstructured Polymer Optical Fibers for High-Temperature-Resistant Fiber Bragg Grating Strain Sensors. *Opt. Mater.* **2016**, *6*, 649–659. [CrossRef]
16. Cennamo, N.; Arcadio, F.; Marletta, V.; Baglio, S.; Zeni, L.; Ando, B. A Magnetic Field Sensor Based on SPR-POF Platforms and Ferrofluids. *IEEE Trans. Instrum. Meas.* **2021**, *70*, 1–10. [CrossRef]
17. Statkiewicz-Barabach, G.; Mergo, P.; Urbanczyk, W. Bragg Grating-Based Fabry–Perot Interferometer Fabricated in a Polymer Fiber for Sensing with Improved Resolution. *J. Opt.* **2016**, *19*, 015609. [CrossRef]
18. Hu, X.; Chen, Y.; Gao, S.; Min, R.; Woyessa, G.; Bang, O.; Qu, H.; Wang, H.; Caucheteur, C. Direct Bragg Grating Inscription in Single Mode Step-Index TOPAS/ZEONEX Polymer Optical Fiber Using 520 Nm Femtosecond Pulses. *Citation* **2022**, *14*, 1350. [CrossRef]
19. Dengler, S.A.; Roseeu, R.V.; Luber, G.M.; Ziemann, O.; Engelbrecht, R.; Schmauss, B. Performance Evaluation of Reference Reflections in Polymer Optical Fibers for Strain Sensing. In Proceedings of the 27th International Conference on Optical Fiber Sensors; Optica Publishing Group: Washington, DC, USA, 2022.
20. Karpienko, K.; Wróbel, M.S.; Jędrzejewska-Szczerska, M. Determination of Refractive Index Dispersion Using Fiber-Optic Low-Coherence Fabry–Perot Interferometer: Implementation and Validation. *Opt. Eng.* **2014**, *53*, 077103. [CrossRef]
21. Hui, R. *Optical Fibers. Introduction to Fiber-Optic Communications*; Elsevier: Amsterdam, The Netherlands, 2020; pp. 19–76. [CrossRef]
22. Saleh, B.E.A.; Teich, M.C. *Fundamentals of Photonics 3rd Edition Part I: Optics Part II: Photonics*; Wiley Series in Pure and Applied Optics; John Wiley & Sons: Hoboken, NJ, USA, 2019; p. 1520.
23. Patil, J.J.; Ghosh, A. Intensity Modulation Based U Shaped Plastic Optical Fiber Refractive Index Sensor. In Proceedings of the 2022 6th International Conference on Trends in Electronics and Informatics, ICOEI, Tirunelveli, India, 28–30 April 2022; pp. 18–24. [CrossRef]
24. Beres, C.; de Nazaré, F.V.B.; de Souza, N.C.C.; Miguel, M.A.L.; Werneck, M.M. Tapered Plastic Optical Fiber-Based Biosensor—Tests and Application. *Biosens. Bioelectron.* **2011**, *30*, 328–332. [CrossRef] [PubMed]

25. Lomer, M.; Galindez, C.A.; Quintela, M.A.; Quintela, A.; Mirapeix, J.; Lopez-Higuera, J.M. Refractometric Sensor Based on Induced Losses in the Region of Transition from a Curved Side-Polished POF Fiber. In Proceedings of the 19th International Conference on Optical Fibre Sensors, Perth, WA, Australia, 16 May 2008; Volume 7004, p. 70045H. [CrossRef]
26. Listewnik, P.; Hirsch, M.; Struk, P.; Weber, M.; Bechelany, M.; Jędrzejewska-Szczerska, M. Preparation and Characterization of Microsphere ZnO ALD Coating Dedicated for the Fiber-Optic Refractive Index Sensor. *Nanomaterials* **2019**, *9*, 306. [CrossRef]
27. Hirsch, M.; Listewnik, P.; Struk, P.; Weber, M.; Bechelany, M.; Szczerska, M. ZnO Coated Fiber Optic Microsphere Sensor for the Enhanced Refractive Index Sensing. *Sens. Actuators A Phys.* **2019**, *298*, 111594. [CrossRef]
28. Felsen, L.B. Evanescent waves. *J. Opt. Soc. Am.* **1976**, *66*, 751–760. [CrossRef]
29. Tan, A.J.Y.; Ng, S.M.; Stoddart, P.R.; Chua, H.S. Theoretical Model and Design Considerations of U-Shaped Fiber Optic Sensors: A Review. *IEEE Sens. J.* **2020**, *20*, 14578–14589. [CrossRef]
30. Chen, K.-C.; Li, Y.-L.; Wu, C.-W.; Chiang, C.-C. Glucose Sensor Using U-Shaped Optical Fiber Probe with Gold Nanoparticles and Glucose Oxidase. *Sensors* **2018**, *18*, 1217. [CrossRef] [PubMed]
31. Memon, S.F.; Wang, R.; Strunz, B.; Chowdhry, B.S.; Pembroke, J.T.; Lewis, E. Novel Corrugated Long Period Grating Surface Balloon-Shaped Heterocore-Structured Plastic Optical Fibre Sensor for Microalgal Bioethanol Production. *Sensors* **2023**, *23*, 1644. [CrossRef] [PubMed]
32. Wang, S.; Zhang, D.; Xu, Y.; Sun, S.; Sun, X. Refractive Index Sensor Based on Double Side-Polished U-Shaped Plastic Optical Fiber. *Sensors* **2020**, *20*, 5253. [CrossRef]
33. Viegas, D.; Abad, S.; Santos, J.L.; Ferreira, L.A.; Araújo, F.M. Non-Terminal Miniature Fiber Bragg Grating Temperature Probe Based in a u-Shape Lossless Taper. *Meas. Sci. Technol.* **2010**, *21*, 094002. [CrossRef]
34. Leffers, L.; Locmelis, J.; Bremer, K.; Roth, B.; Overmeyer, L. Polymer Optical Fibre Bend Sensor Based on Eccentrical Bragg Gratings. In Proceedings of the 2021 Conference on Lasers and Electro-Optics (CLEO), San Jose, CA, USA, 9–14 May 2021; p. STu2F.8. [CrossRef]
35. Tan, A.J.Y.; Ng, S.M.; Stoddart, P.R.; Chua, H.S. Trends and Applications of U-Shaped Fiber Optic Sensors: A Review. *IEEE Sens. J.* **2021**, *21*, 120–131. [CrossRef]
36. Jin, Y.; M Granville, A. Polymer Fiber Optic Sensors—A Mini Review of Their Synthesis and Applications. *J. Biosens. Bioelectron.* **2016**, *7*, 1. [CrossRef]
37. Wandemur, G.; Rodrigues, D.; Allil, R.; Queiroz, V.; Peixoto, R.; Werneck, M.; Miguel, M. Plastic Optical Fiber-Based Biosensor Platform for Rapid Cell Detection. *Biosens. Bioelectron.* **2014**, *54*, 661–666. [CrossRef] [PubMed]
38. Teng, C.; Shao, P.; Li, S.; Li, S.; Liu, H.; Deng, H.; Chen, M.; Yuan, L.; Deng, S. Double-Side Polished U-Shape Plastic Optical Fiber Based SPR Sensor for the Simultaneous Measurement of Refractive Index and Temperature. *Opt. Commun.* **2022**, *525*, 128844. [CrossRef]
39. Johari, S.H.; Cheak, T.Z.; Abdul Rahim, H.R.; Jali, M.H.; Mohd Yusof, H.H.; Md Johari, M.A.; Yasin, M.; Harun, S.W. ZnO Nanorods Coated Tapered U-Shape Plastic Optical Fiber for Relative Humidity Detection. *Photonics* **2022**, *9*, 796. [CrossRef]
40. Tang, Z.; Gomez, D.; He, C.; Korposh, S.; Morgan, S.P.; Correia, R.; Hayes-Gill, B.; Setchfield, K.; Liu, L. A U-Shape Fibre-Optic pH Sensor Based on Hydrogen Bonding of Ethyl Cellulose with a Sol-Gel Matrix. *J. Light. Technol.* **2021**, *39*, 1557–1564. [CrossRef]
41. Yetisen, A.K.; Jiang, N.; Fallahi, A.; Montelongo, Y.; Ruiz-Esparza, G.U.; Tamayol, A.; Zhang, Y.S.; Mahmood, I.; Yang, S.A.; Kim, K.S.; et al. Glucose-Sensitive Hydrogel Optical Fibers Functionalized with Phenylboronic Acid. *Adv. Mater.* **2017**, *29*, 1606380. [CrossRef] [PubMed]
42. Stupar, D.Z.; Bajić, J.S.; Joža, A.V.; Dakić, B.M.; Slankamenac, M.P.; Živanov, M.B.; Cibula, E. Remote Monitoring of Water Salinity by Using Side-Polished Fiber-Optic U-Shaped Sensor. In Proceedings of the 15th International Power Electronics and Motion Control Conference and Exposition, EPE-PEMC 2012 ECCE Europe, Novi Sad, Serbia, 4–6 September 2012. [CrossRef]
43. Johari, S.H.; Cheak, T.Z.; Rahim, H.R.A.; Jali, M.H.; Yusof, H.H.M.; Johari, M.A.M.; Harun, S.W. Formaldehyde Sensing Using Tapered U-Shape Plastic Optical Fiber Coated with Zinc Oxide Nanorods. *IEEE Access* **2022**, *10*, 91445–91451. [CrossRef]
44. Jaiswal, A.K.; Hokkanen, A.; Kapulainen, M.; Khakalo, A.; Nonappa; Ikkala, O.; Orelma, H. Carboxymethyl Cellulose (CMC) Optical Fibers for Environment Sensing and Short-Range Optical Signal Transmission. *ACS Appl. Mater. Interfaces* **2022**, *14*, 3315–3323. [CrossRef]
45. Yee Tan, A.J.; Seng Ung, K.; Ng, S.M.; Stoddart, P.R.; Chua, H.S. Refractive Index, Temperature, and Heat Source Origin Sensing with Dual U-Shaped Fiber Probes. In Proceedings of the 2021 IEEE International Conference on Sensors and Nanotechnology, Port Dickson, Malaysia, 22–24 September 2021; pp. 29–32. [CrossRef]
46. Song, H.; Zhang, H.; Sun, Z.; Ren, Z.; Yang, X.; Wang, Q. Triangular Silver Nanoparticle U-Bent Fiber Sensor Based on Localized Surface Plasmon Resonance. *AIP Adv.* **2019**, *9*, 085307. [CrossRef]
47. Chandra, S.; Dhawangale, A.; Mukherji, S. Hand-Held Optical Sensor Using Denatured Antibody Coated Electro-Active Polymer for Ultra-Trace Detection of Copper in Blood Serum and Environmental Samples. *Biosens. Bioelectron.* **2018**, *110*, 38–43. [CrossRef]

48. George, A.; Amrutha, M.S.; Srivastava, P.; Sunil, S.; Sai, V.V.R.; Srinivasan, R. Development of a U-Bent Plastic Optical Fiber Biosensor with Plasmonic Labels for the Detection of Chikungunya Non-Structural Protein 3. *Analyst* **2021**, *146*, 244–252. [CrossRef] [PubMed]
49. Lee, S.C.J. Discrete Multitone Modulation for Short-Range Optical Communications. Ph.D. Thesis, Technische Universiteit Eindhoven, Eindhoven, The Netherlands, 2009. [CrossRef]
50. Moslan, M.S.; Othman, M.H.D.; Samavati, A.; Salim, M.A.M.; Rahman, M.A.; Ismail, A.F.; Bakhtiar, H. Fabrication of Polycarbonate Polymer Optical Fibre Core via Extrusion Method: The Role of Temperature Gradient and Collector Speed on Its Characteristics. *Opt. Fiber Technol.* **2020**, *55*, 102162. [CrossRef]
51. Beckers, M.; Schlüter, T.; Vad, T.; Gries, T.; Bunge, C.A. An Overview on Fabrication Methods for Polymer Optical Fibers. *Polym. Int.* **2015**, *64*, 25–36. [CrossRef]
52. ESKA Polymer Optical Fiber Technical Data. Available online: https://www.pofeska.com/pofeskae/download/02.html (accessed on 5 January 2025).
53. Zubel, M.G.; Fasano, A.; Woyessa, G.; Sugden, K.; Rasmussen, H.K.; Bang, O. 3D-Printed PMMA Preform for Hollow-Core POF Drawing. In Proceedings of the 25th International Conference on Plastic Optical Fibers, Birmingham, UK, 13–15 September 2016.
54. Ziemann, O.; Krauser, J.; Zamzow, P.E.; Daum, W. *POF Handbook: Optical Short Range Transmission Systems*; John Wiley & Sons, Inc.: Hoboken, NJ, USA, 2008; pp. 1–886. [CrossRef]
55. Pituru, S.M.; Greabu, M.; Totan, A.; Imre, M.; Pantea, M.; Spinu, T.; Tancu, A.M.C.; Popoviciu, N.O.; Stanescu, I.I.; Ionescu, E. A Review on the Biocompatibility of PMMA-Based Dental Materials for Interim Prosthetic Restorations with a Glimpse into Their Modern Manufacturing Techniques. *Materials* **2020**, *13*, 2894. [CrossRef] [PubMed]
56. Ali, U.; Karim, K.J.B.A.; Buang, N.A. A Review of the Properties and Applications of Poly (Methyl Methacrylate) (PMMA). *Polym. Rev.* **2015**, *55*, 678–705. [CrossRef]
57. De Castro Monsores, K.G.; Da Silva, A.O.; Oliveira, S.D.S.A.; Rodrigues, J.G.P.; Weber, R.P. Influence of Ultraviolet Radiation on Polymethylmethacrylate (PMMA). *J. Mater. Res. Technol.* **2019**, *8*, 3713–3718. [CrossRef]
58. Gierej, A.; Filipkowski, A.; Pysz, D.; Buczynski, R.; Vagenende, M.; Dubruel, P.; Thienpont, H.; Geernaert, T.; Berghmans, F. On the Characterization of Novel Step-Index Biocompatible and Biodegradable Poly(D,L-Lactic Acid) Based Optical Fiber. *J. Light. Technol.* **2020**, *38*, 1905–1914. [CrossRef]
59. Omenetto, F.G.; Kaplan, D.L. A New Route for Silk. *Nat. Photonics* **2008**, *2*, 641–643. [CrossRef]
60. Mittal, N.; Jansson, R.; Widhe, M.; Benselfelt, T.; Håkansson, K.M.O.; Lundell, F.; Hedhammar, M.; Söderberg, L.D. Ultrastrong and Bioactive Nanostructured Bio-Based Composites. *ACS Nano* **2017**, *11*, 5148–5159. [CrossRef] [PubMed]
61. CYTOPTM Technical Information—AGC Chemicals Europe. Available online: https://www.agcce.com/cytop-technical-information/ (accessed on 13 December 2023).
62. CYTOP® | Product Information | Fluoroproducts Business | AGC Chemicals Company. Available online: https://www.agc-chemicals.com/jp/en/fluorine/products/detail/index.html?pCode=JP-EN-F019 (accessed on 13 December 2023).
63. Koike, Y.; Koike, K. Optical Fibers. In *Polymer Science: A Comprehensive Reference*; Elsevier: Amsterdam, The Netherlands, 2012; pp. 283–304. [CrossRef]
64. Koike, Y. *Fundamentals of Plastic Optical Fibers*; Wiley-VCH Verlag GmbH 7 Co.: Weinheim, Germany, 2014; pp. 139–168. [CrossRef]
65. Leal-Junior, A.G.; Theodosiou, A.; Díaz, C.R.; Marques, C.; Pontes, M.J.; Kalli, K.; Frizera, A. Simultaneous Measurement of Axial Strain, Bending and Torsion with a Single Fiber Bragg Grating in CYTOP Fiber. *J. Light. Technol.* **2019**, *37*, 971–980. [CrossRef]
66. Nan, Y.-G.; Yazd, N.S.; Chapalo, I.; Chah, K.; Hu, X.; Mégret, P. Properties of Fiber Bragg Grating in CYTOP Fiber Response to Temperature, Humidity, and Strain Using Factorial Design. *Sensors* **2022**, *22*, 1934. [CrossRef] [PubMed]
67. Evertz, A.; Schrein, D.; Olsen, E.; Hoffmann, G.; Overmeyer, L. Dip coating of thin polymer optical fibers. *Opt. Fiber Technol.* **2021**, *66*, 102638. [CrossRef]
68. Zhao, Q.; Tian, F.; Yang, X.; Li, S.; Zhang, J.; Zhu, X.; Yang, J.; Liu, Z.; Zhang, Y.; Yuan, T.; et al. Optical Fibers with Special Shaped Cores Drawn from 3D Printed Preforms. *Optik* **2017**, *133*, 60–65. [CrossRef]
69. Choi, M.; Humar, M.; Kim, S.; Yun, S.H. Step-Index Optical Fiber Made of Biocompatible Hydrogels. *Adv. Mater.* **2015**, *27*, 4081–4086. [CrossRef]
70. Chen, G.; Hou, K.; Yu, N.; Wei, P.; Chen, T.; Zhang, C.; Wang, S.; Liu, H.; Cao, R.; Zhu, L.; et al. Temperature-Adaptive Hydrogel Optical Waveguide with Soft Tissue-Affinity for Thermal Regulated Interventional Photomedicine. *Nat. Commun.* **2022**, *13*, 7789. [CrossRef]
71. Parker, S.T.; Domachuk, P.; Amsden, J.; Bressner, J.; Lewis, J.A.; Kaplan, D.L.; Omenetto, F.C. Biocompatible Silk Printed Optical Waveguides. *Adv. Mater.* **2009**, *21*, 2411–2415. [CrossRef]
72. Woyessa, G.; Rasmussen, H.K.; Bang, O. Zeonex—A Route towards Low Loss Humidity Insensitive Single-Mode Step-Index Polymer Optical Fibre. *Opt. Fiber Technol.* **2020**, *57*, 102231. [CrossRef]
73. Zoetex Chemical Resistance. Available online: https://www.zeonex.com/pharmaceuticals.aspx.html (accessed on 7 February 2023).

74. Woyessa, G.; Fasano, A.; Markos, C.; Rasmussen, H.K.; Bang, O. Zeonex Microstructured Polymer Optical Fibre Bragg Grating Sensor. In *Photonics and Fiber Technology 2016 (ACOFT, BGPP, NP)*; Optica Publishing Group: Washington, DC, USA, 2016; p. AW3C.4. [CrossRef]
75. Woliński, T.R.; Mileńko, K.; Tefelska, M.M.; Rutkowska, K.A.; Domański, A.W.; Ertman, S.; Orzechowski, K.; Sierakowski, M.; Chojnowska, O.; Dąbrowski, R. Liquid Crystals and Polymer-Based Photonic Crystal Fibers. *Mol. Cryst. Liq. Cryst.* **2014**, *594*, 55–62. [CrossRef]
76. Inglev, R.; Møller, E.; Højgaard, J.; Bang, O.; Janting, J. Optimization of All-Polymer Optical Fiber Oxygen Sensors with Antenna Dyes and Improved Solvent Selection Using Hansen Solubility Parameters. *Sensors* **2021**, *21*, 5. [CrossRef] [PubMed]
77. Pires, R.A.; Pashkuleva, I.; Reis, R.L. *Multifunctional Hydrogels for Biomedical Applications*; John Wiley & Sons, Inc.: Hoboken, NJ, USA, 2022.
78. Reimer, M.; Van Opdenbosch, D.; Zollfrank, C. Fabrication of Cellulose-Based Biopolymer Optical Fibers and Their Theoretical Attenuation Limit. *Biomacromolecules* **2021**, *22*, 3297–3312. [CrossRef] [PubMed]
79. Woyessa, G.; Fasano, A.; Stefani, A.; Markos, C.; Nielsen, K.; Rasmussen, H.K.; Bang, O.; Dobb, H.; Webb, D.J.; Kalli, K.; et al. Single Mode Step-Index Polymer Optical Fiber for Humidity Insensitive High Temperature Fiber Bragg Grating Sensors. *Opt. Express* **2016**, *24*, 1253–1260. [CrossRef]
80. Ahmed, I.; Ali, M.; Elsherif, M.; Butt, H. UV polymerization fabrication method for polymer composite based optical fiber sensors. *Sci. Rep.* **2023**, *13*, 10823. [CrossRef]
81. Reimer, M.; Mayer, K.; Van Opdenbosch, D.; Scheibel, T.; Zollfrank, C. Biocompatible Optical Fibers Made of Regenerated Cellulose and Recombinant Cellulose-Binding Spider Silk. *Biomimetics* **2023**, *8*, 37. [CrossRef] [PubMed]
82. MatWeb Material Property Data. Available online: https://www.matweb.com/search/DataSheet.aspx?MatGUID=632572aeef2a4224b5ac8fbd4f1b6f77&ckck=1 (accessed on 5 January 2025).
83. He, R.; Teng, C.; Kumar, S.; Marques, C.; Min, R. Polymer Optical Fiber Liquid Level Sensor: A Review. *IEEE Sens. J.* **2022**, *22*, 1081–1091. [CrossRef]
84. Arcas, A.D.S.; Dutra, F.D.S.; Allil, R.C.S.B.; Werneck, M.M. Surface Plasmon Resonance and Bending Loss-Based U-Shaped Plastic Optical Fiber Biosensors. *Sensors* **2018**, *18*, 648. [CrossRef]
85. Rashid, A.R.A.; Hakim, A.A.N.; Yahaya, N.; Surani, A.H. U-Bent Polymer Optical Fiber (POF) for Escherichia Coli Detection. *Optoelectron. Adv. Mater. Rapid Commun.* **2020**, *14*, 118–122.
86. Okazaki, T.; Kamio, H.; Yoshioka, M.; Ueda, A.; Kuramitz, H.; Watanabe, T. U-Shaped Plastic Optical Fiber Sensor for Scale Deposition in Hot Spring Water. *Anal. Sci.* **2022**, *38*, 1549–1554. [CrossRef] [PubMed]
87. Reimer, M.; Zollfrank, C. Cellulose for Light Manipulation: Methods, Applications, and Prospects. *Adv. Energy Mater.* **2021**, *11*, 2003866. [CrossRef]
88. Godbout, N.; Guo, N.; Gao, Y.; Dubois, C.; Dupuis, A.; Skorobogatiy, M.; Lacroix, S. Prospective for Biodegradable Microstructured Optical Fibers. *Opt. Lett.* **2007**, *32*, 109–111. [CrossRef]
89. Zhao, Y.; Peng, Y.; Chen, M.-Q.; Xia, F.; Tong, R.-J. U-Shaped Microfiber Coupler Coated with Polyvinyl Alcohol Film for Highly Sensitive Humidity Detection. *Sens. Actuators A Phys.* **2019**, *285*, 628–636. [CrossRef]
90. Wen, H.Y.; Hsu, H.C.; Tsai, Y.T.; Feng, W.K.; Lin, C.L.; Chiang, C.C. U-Shaped Optical Fiber Probes Coated with Electrically Doped GQDs for Humidity Measurements. *Polymers* **2021**, *13*, 2696. [CrossRef]
91. Dante, A.; Silva, P.H.; Lopes, R.; Allil, A.; Sbano, A.; Esteves, M.E.; Silva, M.; Werneck, M.; Allil, R. Development of an Escherichia Coli Optical Biosensor with Computational Validation. *J. Phys. Conf. Ser.* **2022**, *2407*, 012029. [CrossRef]
92. Zhang, R.; Du, F.; Jariyavidyanont, K.; Zhuravlev, E.; Schick, C.; Androsch, R. Glass Transition Temperature of Poly(D,L-Lactic Acid) of Different Molar Mass. *Thermochim. Acta* **2022**, *718*, 179387. [CrossRef]
93. Elsherif, M.; Umair Hassan, M.; Yetisen, A.K.; Butt, H. Hydrogel Optical Fibers for Continuous Glucose Monitoring. *Biosens. Bioelectron.* **2019**, *137*, 125–132. [CrossRef]
94. Rekowska, N.; Arbeiter, D.; Konasch, J.; Riess, A.; Mau, R.; Eickner, T.; Seitz, H.; Grabow, N.; Teske, M. Thermomechanical properties of PEGDA and its co-polymers. *Curr. Dir. Biomed. Eng.* **2018**, *4*, 669–672. [CrossRef]
95. Szczerska, M. Temperature Sensors Based on Polymer Fiber Optic Interferometer. *Chemosensors* **2022**, *10*, 228. [CrossRef]

Disclaimer/Publisher's Note: The statements, opinions and data contained in all publications are solely those of the individual author(s) and contributor(s) and not of MDPI and/or the editor(s). MDPI and/or the editor(s) disclaim responsibility for any injury to people or property resulting from any ideas, methods, instructions or products referred to in the content.